

Optical training of large-scale Transformers and deep neural networks with direct feedback alignment

Ziao Wang^{1,*}, Kilian Müller^{2,3,*}, Matthew Filipovich^{2,4}, Julien Launay², Ruben Ohana^{2,5}, Gustave Pariente², Safa Mokaadi², Charles Brossollet², Fabien Moreau², Alessandro Cappelli², Iacopo Poli², Igor Carron², Laurent Daudet², Florent Krzakala⁶, and Sylvain Gigan^{1,†}

¹*Laboratoire Kastler Brossel, École Normale Supérieure - Université PSL, Sorbonne Université, Collège de France, CNRS, UMR 8552, Paris, France.*

²*LightOn, 2 rue de la Bourse, 75002 Paris, France.*

³*Welinq, 14 rue Jean Macé, 75011 Paris, France.*

⁴*Clarendon Laboratory, University of Oxford, Parks Road, OX1 3PU, Oxford, United Kingdom.*

⁵*Center for Computational Mathematics, Flatiron Institute, New York, USA.*

⁶*École Polytechnique Fédérale de Lausanne (EPFL), Information, Learning and Physics lab, CH-1015 Lausanne, Switzerland.*

* These authors contributed equally to the work

† Email: sylvain.gigan@lkb.ens.fr

Modern machine learning relies nearly exclusively on dedicated electronic hardware accelerators. Photonic approaches, with low consumption and high operation speed, are increasingly considered for inference but, to date, remain mostly limited to relatively basic tasks. Simultaneously, the problem of training deep and complex neural networks, overwhelmingly performed through backpropagation, remains a significant limitation to the size and, consequently, the performance of current architectures and a major compute and energy bottleneck. Here, we experimentally implement a versatile and scalable training algorithm, called direct feedback alignment, on a hybrid electronic-photonic platform. An optical processing unit performs large-scale random matrix multiplications, which is the central operation of this algorithm, at speeds up to 1500 TeraOps. We perform optical training of one of the most recent deep learning architectures, including Transformers, with more than 1B parameters,

and obtain good performances on both language and vision tasks. We study the compute scaling of our hybrid optical approach, and demonstrate a potential advantage for ultra-deep and wide neural networks, thus opening a promising route to sustain the exponential growth of modern artificial intelligence beyond traditional von Neumann approaches.

1 Introduction

After decades of dominance by the Central Processing Unit (CPU) for computing all kinds of tasks, the emergence of deep learning has triggered the development of specialized hardware. Important examples of hardware specialization are the evolution of GPUs and the development of TPUs, both containing small but numerous processing cores, allowing them to leverage parallelization in tasks like vector-matrix multiplications that are central to today’s machine learning algorithms. All these computing architectures are built upon digital hardware that follows the von Neuman paradigm ¹, and the performances are fundamentally intertwined with the hardware and algorithms ².

Optics is a promising alternative computing architecture: Except under special circumstances, the propagation of light is linear and can therefore be described by a matrix that connects the input and the output fields. In other words, the propagation of light solves a vector-matrix multiplication, and it does so entirely passively, and wholly in parallel. The latter point suggests that the equivalent of the computational complexity of a vector-matrix multiplication of $O(N^2)$ on traditional hardware is reduced to $O(1)$. Practically, the finite communication bandwidth between a computer and the optical processor imposes a scaling of $O(N)$ to the speed at which data can be processed, dictated by the size of the input and output vectors. These favorable properties and the importance of this mathematical operation in data science and machine learning are the reasons for the continuous research in optical computing. However, despite these promises, optical computing today remains limited to relatively small toy tasks and, therefore, does not fully take advantage of this favorable scaling, and lags behind in the current race for more efficient hardware for deep learning.

Whatever their physical implementation, most artificial neural networks (ANNs) are to date trained with end-to-end back-propagation (BP) of the error ^{3–5}, even when implemented on physical hardware ⁶. An error is derived from the network prediction (e.g., from a supervised classification task or an unsupervised generative reconstruction task) and is used as a feedback signal to obtain parameter updates by inverting forward computations through the chain rule of derivatives. Despite decades of continuous improvement, BP bears some limitations. It is fundamentally sequential and enforces *backward locking* ⁷: a given layer may only be updated if the subsequent layer has already completed both its forward and backward pass. This hampers simple and efficient parallelization of extreme-scale models. Even with model, data, and pipeline parallelism schemes ^{8,9}, GPU throughput during training remains bound by data transfer rates ¹⁰. Alternatives to BP have, however, mainly been studied under the guise of *biological realism* ¹¹, seeking to alleviate issues such as the weight transport problem ^{12,13}. Local learning schemes with more practical considerations have been proposed but still remain of marginal use ^{14,15}.

In contrast to the sequential layer updates of BP, Direct Feedback Alignment (DFA) ¹⁶ uses a random projection of the error as a direct feedback signal for each layer, converting the backward pass into an entirely parallel process. DFA enables learning by approximating BP updates through a process known as alignment: forward weights eventually learn to approximate a configuration that makes the randomized feedback useful ¹⁷. Among alternative training methods, DFA stands out in two ways: (1) it scales to modern deep learning tasks and architectures ¹⁸, which is rarely the case in alternative training methods ¹⁹; (2) it places a single operation (a random projection) at the center-stage of training. In previous numerical studies, we have established best practices on how to use DFA ²⁰, and shown that DFA can be applied to modern deep learning tasks and architectures and finally discuss the limits of this algorithm when compared to back-propagation ²¹.

In this work, we leverage the fact that large-scale random projections can naturally be performed optically by exploiting multiple scattering of light ^{22,23}. We therefore use an Optical Processing Unit (OPU) as a hardware accelerator that is perfectly matched to the DFA algorithm, as it improves the computational complexity scaling of the single operation that is its major com-

putational bottleneck. Preliminary studies to implement DFA with optics hardware have so far focused on small-scale proof-of-concept and basic networks^{24,25}. In the present work, we show that this combination of hardware and algorithm can train multiple types of digital ANNs, including Transformers and fully connected deep neural nets, and that it can scale to more than one billion parameters, by far a record in non-conventional hardware training methods. The trained models demonstrate excellent final performances across diverse tasks, from language models to complex climate projections. Finally, we study the scaling performance in terms of training time, showing that our optical training approach may provide a significant speedup for ultra-deep and ultra-large networks in the future.

2 Artificial Neural Network Training on an Optical Processor

Our OPU^{22,23} is based on free space optics, with the light propagating in three-dimensional space, which allows it to make the best use of the parallelism and scaling of optical computation. We use the fact that a complex medium, in which light is randomly and coherently scattered multiple times, naturally leads to a transmission matrix with random entries drawn from a normal distribution²⁷. Such matrices are surprisingly versatile: the field of Randomized Numerical Linear Algebra (RNLA), for example, exploits their properties to tackle high-dimensional problems^{28–30}. We have previously explored how our OPU is a natural hardware match to these RNLA algorithms³¹, and showed that it can perform different ML tasks^{32–35}. Our OPU can handle input and output vectors with dimensions up to 1×10^6 and 2×10^6 , respectively. At this resolution, the maximum frequency is 340 Hz.

A schematic representation of the OPU is shown in Fig. 1: A DMD (Digital Micromirror Device) modulates the incoming light field and, therefore, controls the input vector x of the calculation. DMDs allow the change of this input vector at kHz rates but only permit binary amplitude modulation. That is, the input vector x can only contain the elements 0 and 1. The complex medium gives rise to a random transmission matrix \mathbf{T} . Finally, the camera captures the intensity $|y|^2 = |\mathbf{T}x|^2$ of the output field y . We further exploit two additional features. We first implement

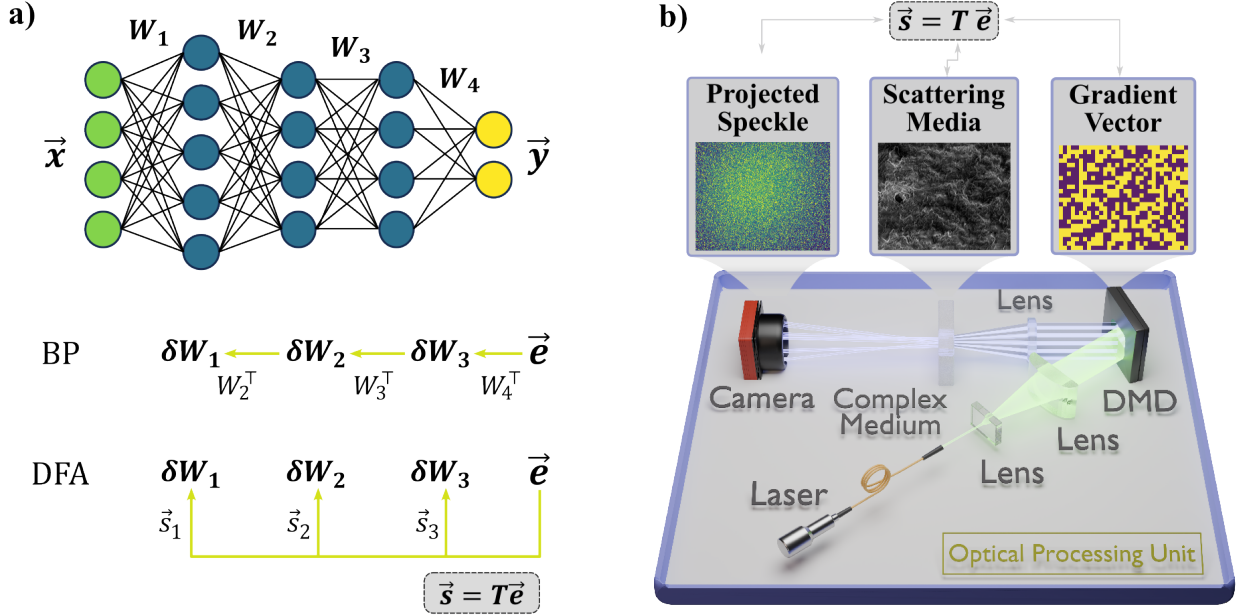


Figure 1: Overview of the direct feedback alignment (DFA) algorithm and Optical Processing Unit (OPU). **a**, Concept of the direct feedback error propagation configuration. Back-propagation (BP) propagates the error \vec{e} sequentially from the last layer to the first, while DFA propagates the error in a parallel way to all layers, with randomly projected signals. **b**, Illustration of the OPU. Coherent laser light illuminates a spatial light modulator (DMD), propagates through a strongly scattering medium, and is detected on a camera. The error vector \vec{e} is ternarized-encoded into binary pixels on the DMD and then propagates through a diffusive medium, effectively performing $T\vec{e}$, a random projection on the fields with T a large complex gaussian and fixed random matrix. While the camera records an intensity pattern $|y|^2 = |Tx|^2$ that depends non-linearly on the input vector x , linear random projections can be recovered thanks to the encoding strategy 26. A dedicated FPGA board controls the photonic core, synchronizing the DMD and camera. The user interfaces with the OPU through a Python library, which is directly compatible with Numpy and PyTorch data types.

a method to obtain linear random projections from such intensity measurements without holography²⁶. Secondly, we ternarize the input data into vectors containing only $\{-1, 0, 1\}$, which comes at no discernible performance loss when using the DFA algorithm. Separate random projections of the positive and negative parts are combined in a post-processing step.

3 Training a generative Transformer on natural language processing

To demonstrate the feasibility of the proposed hybrid approach, we employed optical DFA (ODFA, see SI Note 1) to train a Transformer with 1.07 billion parameters (comparable to GPT2³⁶). Among the parameters of the decoder blocks of the Transformer architecture, 400M parameters directly received the optical signals as the gradients (see SI Note 3). We trained this Transformer on the Cornell Movie-Dialogs Corpus³⁷, which consists of the characters' names and their conversations. We divided the corpus of texts into $\sim 1.2 \times 10^6$ sub-word tokens (i.e., the dataset size) which are composed of 1016 unique tokens (i.e., the vocabulary size). Given a sequence of tokens as the input (context), a generative Transformer for natural language processing determines the next token by calculating the probability of each token in the vocabulary. While the inference of Transformers with optics has been investigated³⁸, training optically remains unexplored.

Figure 2a shows the architecture of the Transformer we trained using ODFA, and panel b depicts a schematic drawing of our OPU. Panel c shows the loss trajectories to compare different training methods. Aside from ODFA, DFA, and BP, we added one Shallow Training (SHLW) baseline to validate that the optical signals delivered by ODFA are indeed conveying learning to the layers. One can observe that over two training epochs, all the training methods enable Transformers to learn the probability distribution of the vocabulary, as shown by the continuously decreasing loss trajectories. We can also observe that the final losses of BP and DFA are at the same level (see SI Note 3 for further discussion) and that ODFA, while it learns somewhat more slowly, still shows a consistent learning pace throughout the training with the same configuration. As a concrete example, the ODFA-trained Transformer was provided with a prompt, “JACK: The problem is not the problem. The problem is your attitude about the problem.” The generated

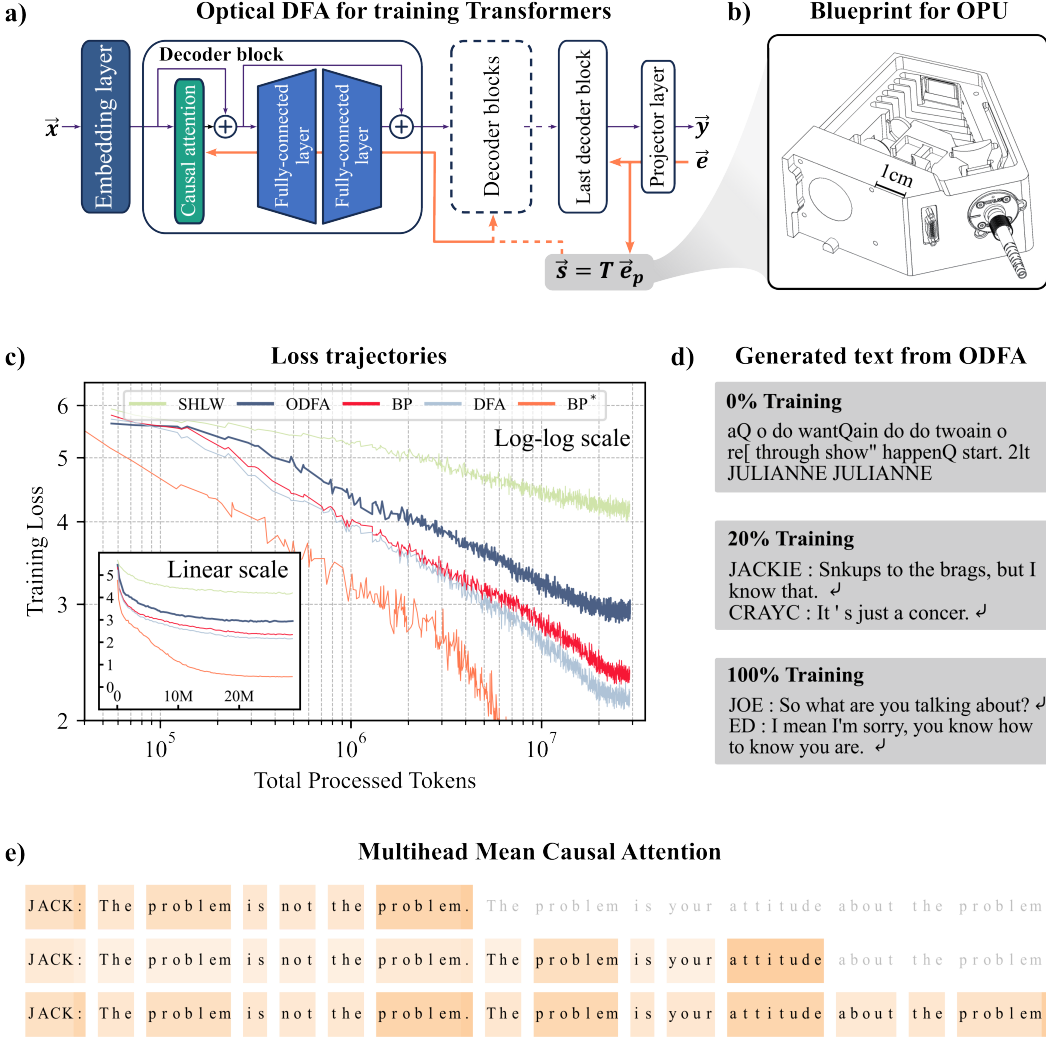


Figure 2: Optical training of a generative Transformer for Movie-DIALOGS dataset. **a**, Schematic representation of our optical DFA (ODFA) training algorithm. The gradient vector \vec{e}_p from the last layer is multiplied by a random matrix \mathbf{T} and sent to each decoder block other than the last one in parallel with no gradient communication among decoder blocks. **b**, Schematic depiction of our OPU. **c**, Loss trajectories of the generative Transformers trained using various methods. All five methods employed the same architecture, but the first four utilized the same ODFA-adopted training configuration. BP* applied a distinct one where backpropagation can reach the best performance. SHLW trained the last decoder layer solely using backpropagation, with the other parameters frozen (Details in SI Note). **d**, Examples of text generated by the ODFA-trained Transformer at 0%, 20%, and 100% training stages respectively. A bent arrow represents the generated newline token. **e** Mean causal attention for a given prompt as it is fed into the Transformer (at 100% training). We used causal attention, meaning that the tokens in the sequence only incorporate themselves and the previous tokens. The translucent words indicate that the Transformer has not yet processed the tokens. Shades of orange represent the level of attention weight on certain words.

text (Fig. 2d) was observed at different stages of the training process. Initially, the Transformer generated nonsensical combinations of sub-words and punctuations. As the training progressed, the Transformer learned to generate text in a more conversational format, with capital character names at the start of each line, one newline command at the end, and increasingly meaningful words and phrases.

For this proof-of-concept, we adjusted the Transformer parameters to minimize the number of optical projections. In particular, we used a much shorter context length (24 tokens instead of the usual ~ 1000 tokens) and a larger embedding dimension (2040 instead of the conventional ~ 500) (see SI Note 3). Increasing the embedding dimension did not lead to a longer processing time for the OPU. As a result, the quality of the text generated by the ODFA method remains behind the state of the art. This low quality is principally due to the limited context length, which limits the ability to manage long sentences and dialogues: the generated text tends to lack logical connections between utterances. The choice to limit context size is due to the number of optical projections scaling linearly with the number of tokens and the context size. To complete the training within a reasonable time (about 20 hours for ODFA compared to approximately 2 hours with conventional BP in the same configuration), we thus trained the model on a small corpus and reduced context size. Note that the scale of the random projection for language tasks (typically 10^3 inputs to 10^3 outputs) was still limited with respect to the potential dimension of the OPU (10^6 inputs and outputs), resulting in a comparatively slower rate of random projection on the OPU relative to the GPU at this scale. Therefore, we concentrate here on demonstrating the ability of ODFA to train a large-scale Transformer architecture and not on its sheer performance or speed. That being said, the large dimension of the OPU is potentially well adapted for frontier models, whose vocabulary sizes are often in the range of 10^5 , inner model dimensions typically reach 10^4 for dense models, and effectively 10^5 for Mixture-of-Experts like GPT-4³⁹.

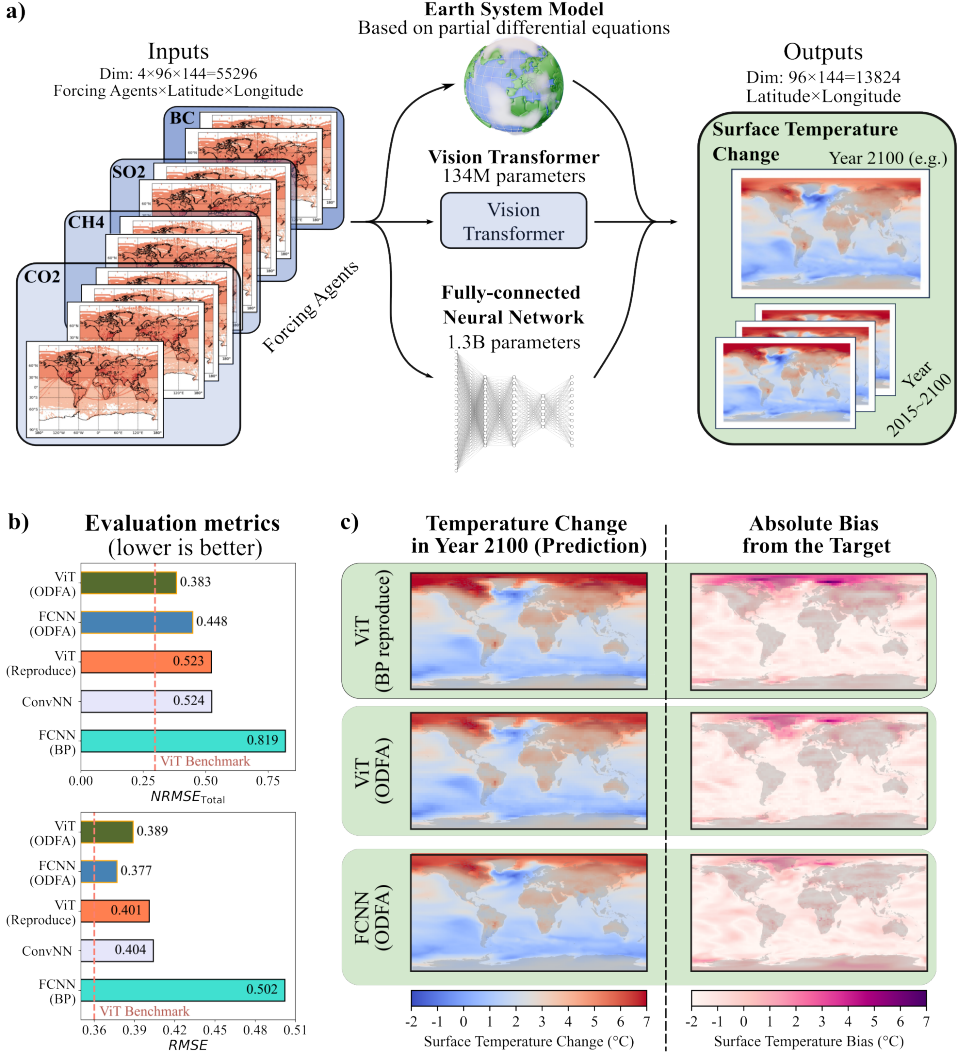


Figure 3: ODFA training of ViT and FCNN on the high dimensional climate projection dataset. a, Schematic illustration of BP/ODFA-trained ViT/FCNN on the climate projection dataset. The inputs are the global distributions of four forcing factors (carbon dioxide, etc.) from 2015 to 2100, with a dimension of 55.3k. The outputs are the global distributions of surface air temperature at certain years, with a dimension of 13.8k. The dataset contains both historical recordings for past years and simulation results based on earth system models for future years. One ViT with 134M parameters and one FCNN with 1.3B parameters were trained both using BP and ODFA. **b**, Performances of BP/ODFA-trained models over two RMSE-based metrics. The BP results of *ViT(Reproduce)* were obtained using the same configuration as *ViT(ODFA)*, and the results of *ConvNN* are from ⁴⁰. Details about the metrics can be found in the SI Note 4. The ViT benchmark (dashed red line) corresponds to optimal training of the ViT using a much larger dataset ⁴¹. **c**, Predictions (left) and absolute bias to the targets(right) of different models on the temperature change in Year 2100. The three rows exhibit the results from ViTs trained by BP, ODFA, and an FCNN trained by ODFA, respectively.

4 Vision Transformer and deep neural networks on climate task

To further test the effectiveness of ODFA in configurations that play more to its strengths, we trained a Vision Transformer (ViT), a type of Transformer that adapts its architecture to computer vision tasks, on the climate projection dataset ClimateBench⁴⁰. Given the heterogeneity of climate projection data sources and the complex nature of the input and output data, the ViT has been identified as an effective model for the task⁴¹. Here, the ViT was optically trained to map and predict the global distributions of four anthropogenic forcing factors to the distribution of the earth’s surface air temperature, with large input and output dimensions of 55296 and 13824, respectively (Fig. 3a). Among 200 million parameters of the ViT, 134 million parameters directly received the ODFA signal. As shown in Fig. 3b, utilizing ODFA to train the ViT delivered the predictions as well as training through backpropagation, according to the four main evaluation metrics of the dataset. The earth’s surface air temperature change predicted by the ODFA-trained ViT closely resembles the target distribution (Fig. 3c). Notably, for this specific task the ODFA method overcame the large performance gap between electronics and optics that we observed in the language task. Indeed, our ODFA-trained ViT is close to the state-of-the-art ViT benchmark model⁴¹.

Next, to highlight the capability of ODFA to train different types of architectures, we trained a fully connected neural network (FCNN) on the same dataset. The architecture of the FCNN in this study consists of 4 layers, with the number of nodes decreasing in the deeper layers and a total of 1.3 billion parameters. For consistency, the last layer was again trained by BP. During training, the gradients from the last layer were optically projected onto the ODFA signal and subsequently sent in parallel to the other layers. Here, 1.03 billion parameters directly received the ODFA signal.

Figure 3b summarizes the evaluation metrics of BP and ODFA. Here, the BP-trained FCNN performed much worse than the ODFA-trained one. The gain in performance can be attributed in part to the training configurations during the backward pass. For such a wide dimensional layer, the gradients in the backward pass require additional task-specific normalization and careful adjustments of the step size and batch size. In practice, Layer Normalization is sometimes used in

the forward pass to re-center and re-scale the gradient in the backward pass ⁴². However, the optical projected signal is naturally normalized throughout the laser and camera calibration: ensuring the camera is not over-exposed naturally leads to a normalized ODFA signal. Therefore, for FCNN, an ODFA-adopted training configuration can lead to an unexpected result for using BP.

5 Scaling towards extreme-scale models

Scaling up machine learning models has emerged as a possible way to improve their performances ⁴³, but it is challenging and expensive due to the heavy compute budget. To further explore the potential of our hybrid optical training method, we here study how the training time for ODFA and BP scale (for the same number of epochs) for fully connected neural networks of increasing dimensions and randomly generated dummy datasets. Note that the loss after a given number of epochs between BP and DFA is different, with an advantage for BP, and thus, a comprehensive comparison in terms of final performance would require further study. Here, to ensure a fair comparison of the training time (in GPU seconds), we measured the total time required to complete the whole training process, which generally involves the forward pass, error vector calculation, gradient or projected signal propagation, and parameter update. For ODFA, we also took into account the training time, the conversion of the digital gradient into an optical signal, the projection time through the scattering medium, the acquisition of the projected signal, and their conversion back into digital representations. As discussed below, the results summarized in Fig. 4 show that DFA, in combination with an optical accelerator, can scale to massive sizes. They also demonstrate that the scaling pre-factors are smaller for ODFA than for BP and therefore hint at a speed advantage compared to pure in-silico GPU training for the largest NNs.

Specifically, in Fig. 4a, we varied the dimension of the hidden layers (number of neurons in each hidden layer) while leaving the numbers of layers fixed, corresponding to a quadratically increasing number of parameters (weights) of neural networks with the number of neurons. When the dimension of the hidden layers is small, BP can process training quickly, in microseconds per sample, for any number of layers. Logically, we nevertheless observed the expected quadratic

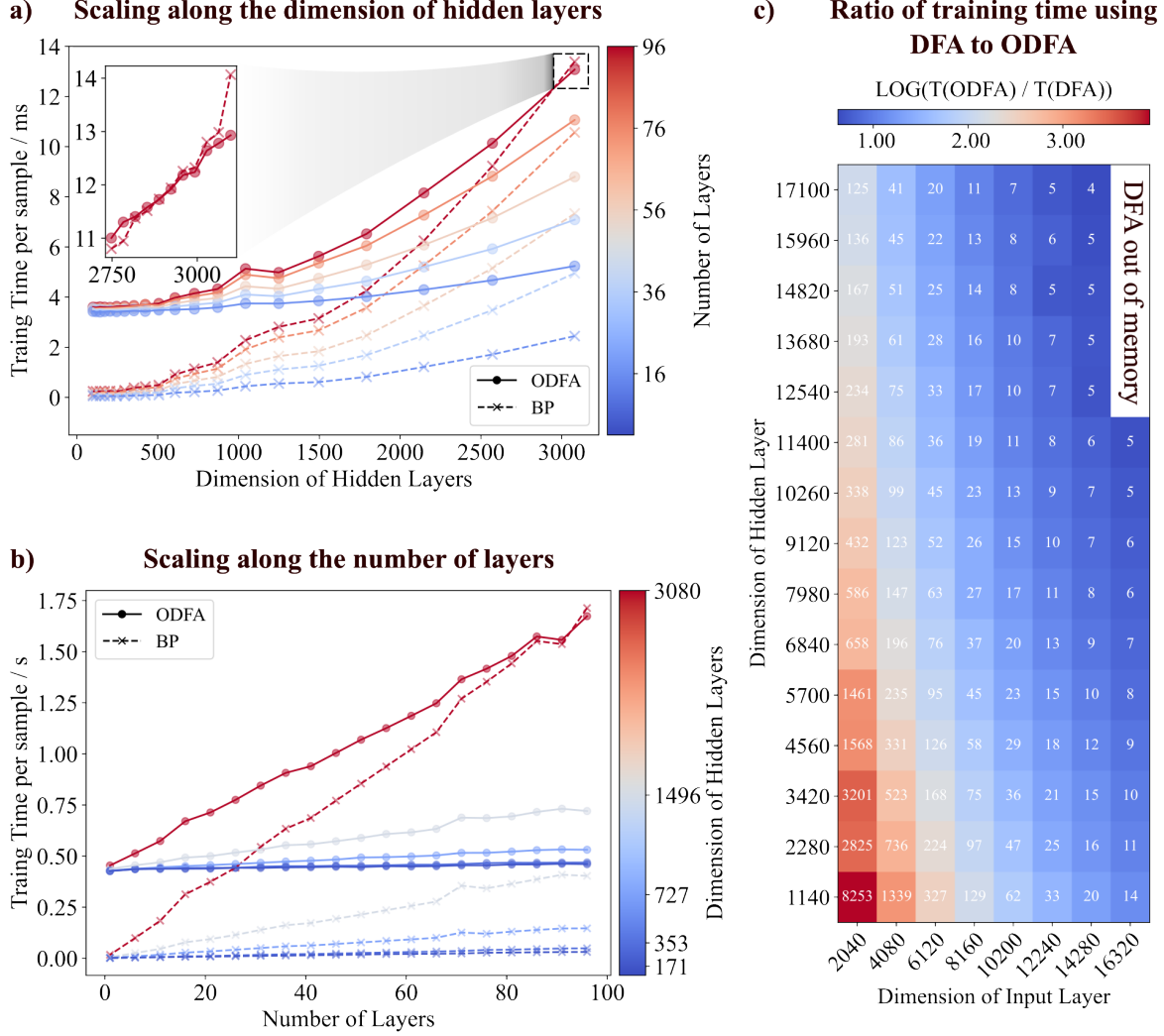


Figure 4: Scaling of the training time for ODFA-trained extreme-scale FCNNs. **a**, Comparison of the training time along the dimension of hidden layers varying from 100 to 3080. The trajectories with dot markers were trained using ODFA, and cross markers were trained using BP. Both follow the expected quadratic behavior. The colors of the curves represent the number of hidden layers, where red indicates a deep and blue a shallow FCNN. At the largest dimension (marked by a star, with 96 hidden layers and 3080 neurons in each hidden layer), using BP (13.39ms per sample) is slower than using ODFA (13.09ms per sample) for our hardware setup. More data points around the crossover region are shown in the inset. **b**, Comparison of the training time along the number of layers varying from 1 to 96. Dimensions of the hidden layer are color-coded, with red indicating a wide FCNN and blue indicating a narrow one. We observe the linear increase of training time with the number of hidden layers. **c**, Ratios of the training time using the OPU (ODFA) and running the DFA algorithm exclusively on the GPU. We observe the time difference between ODFA and DFA narrowing towards higher dimensions before our GPU runs out of memory.

growth of the training time as the dimension grows. For ODFA, the frame rate of the DMD and the camera both set a minimum training time of a few ms, even for a minuscule model. While the ODFA part is independent of the dimension, the update of the parameters and the forward pass remains quadratic. However, the advantage of ODFA becomes significant in the extreme-scale region, where the weight update of BP becomes dominant. Conversely, in Fig. 4b, for a fixed dimension of the hidden layers, we can observe the linear scaling of the training time for BP with the number of layers commensurate with the scaling of the number of parameters of the network. As expected from the scaling of parameters, where increasing the number of layers leads to a linearly increasing number of parameters, the training time for both methods rises with a nearly constant slope. However, the optical method always has a smaller slope again thanks to the $O(1)$ scaling of the random projections with the number of parameters. Ultimately, we can reach a regime where the training speed of ODFA surpasses BP in our case (for 96 layers and 3080 neurons in each layer).

Let us now focus on this training time reduction, which is both due to the algorithm itself, and to the use of optical hardware. The DFA algorithm bypasses the protracted gradient propagation through layers in the backward pass and increases the parallelization. The expected reduction of the training time for certain epochs is around 24% at massive scales. However, this reduction does not exclusively stem from the algorithm. Considering the maximum computing dimension for our optical hardware ($10^6 \times 10^6$) and the dimension of the current gradient projection ($10^3 \times 10^3$), the optical hardware is far from working at its full potential. The projection dimension only depends on the output layer dimension and the largest hidden layer dimension. Fig. 4c shows the decreasing ratio of the DFA training time with and without the OPU for different projection dimensions. The ratio decreases dramatically from 10^4 at the scale of $10^3 \times 10^3$ to around 5 at $10^4 \times 10^4$. Beyond this point, training a larger architecture with BP or DFA will exceed the storage capacity of our GPU, NVIDIA A6000, with 32GB of storage. However, since the coefficients of the large random matrix are stored optically, ODFA can scale beyond DFA's dimensions without much speed penalty (See further discussion in SI Note 1).

6 Discussion

We have presented a symbiotic pairing of non-standard hardware (optics) and training algorithm (direct feedback alignment, DFA) to train large-scale artificial neural networks. We have demonstrated the versatility of this system by training GPT-like models and fully connected neural networks on language and vision tasks. Further, we have shown its scalability by training up to 1B parameters, which to our knowledge is a record for any training scheme using non-conventional hardware.

The fundamental motivation for this work is the promise that pairings between specialized hardware and algorithms can provide pathways outside of the existing “hardware lottery” ². The compelling advantage of our system is its ability to execute the central calculation of the DFA algorithm (a random vector-matrix multiplication) optically for a very large dimension N and within a favorable $O(N)$ time complexity and energy consumption scaling. We have demonstrated this scaling and compared it to the $O(N^2)$ scaling of traditional hardware (GPU) by adapting neural network architectures to the specific strengths of our system. A single one of our current Optical Processing Units (OPU), which is based on free space optics, is capable of processing input and output vectors with $N \sim 10^6$ entries, which is an order of magnitude larger than the requirement of current frontier models. With available off-the-shelf components (SLMs and cameras), N could be increased by another order of magnitude. These properties of optical computation (scaling and large N), combined with the highly parallelizable DFA algorithm hint at the possibility of training extremely large models with a substantial computational advantage. Our approach may therefore provide a sustainable pathway for the training of more capable models, simply through an increase in the number of parameters and the adaptation of the ANN’s architecture to the strengths of the ODFA system.

References

1. Von Neumann, J. First draft of a report on the edvac. *IEEE Annals of the History of Computing* **15**, 27–75 (1993).
2. Hooker, S. The hardware lottery. *arXiv preprint arXiv:2009.06489* (2020).
3. Linnainmaa, S. The representation of the cumulative rounding error of an algorithm as a taylor expansion of the local rounding errors. *Master's Thesis (in Finnish), Univ. Helsinki* 6–7 (1970).
4. Werbos, P. J. Applications of advances in nonlinear sensitivity analysis. In *System modeling and optimization*, 762–770 (Springer, 1982).
5. LeCun, Y., Bengio, Y. & Hinton, G. Deep learning. *Nature* **521**, 436–444 (2015).
6. Wright, L. G. *et al.* Deep physical neural networks trained with backpropagation. *Nature* **601**, 549–555 (2022).
7. Jaderberg, M. *et al.* Decoupled neural interfaces using synthetic gradients. In *International Conference on Machine Learning*, 1627–1635 (PMLR, 2017).
8. Shoeybi, M. *et al.* Megatron-lm: Training multi-billion parameter language models using model parallelism. *arXiv preprint arXiv:1909.08053* (2019).
9. Rasley, J., Rajbhandari, S., Ruwase, O. & He, Y. Deepspeed: System optimizations enable training deep learning models with over 100 billion parameters. In *Proceedings of the 26th ACM SIGKDD International Conference on Knowledge Discovery & Data Mining*, 3505–3506 (2020).
10. Ivanov, A., Dryden, N., Ben-Nun, T., Li, S. & Hoefler, T. Data movement is all you need: A case study on optimizing transformers. In *Pre-Proceedings of Machine Learning and Systems*, vol. 3 (2020).
11. Lillicrap, T. P., Santoro, A., Marris, L., Akerman, C. J. & Hinton, G. Backpropagation and the brain. *Nature Reviews Neuroscience* **21**, 335–346 (2020).

12. Grossberg, S. Competitive learning: From interactive activation to adaptive resonance. *Cognitive science* **11**, 23–63 (1987).
13. Lillicrap, T. P., Cownden, D., Tweed, D. B. & Akerman, C. J. Random synaptic feedback weights support error backpropagation for deep learning. *Nature communications* **7**, 1–10 (2016).
14. Nøkland, A. & Eidnes, L. H. Training neural networks with local error signals. In *International Conference on Machine Learning*, 4839–4850 (PMLR, 2019).
15. Laskin, M. *et al.* Parallel training of deep networks with local updates. *arXiv preprint arXiv:2012.03837* (2020).
16. Nøkland, A. Direct feedback alignment provides learning in deep neural networks. In Lee, D., Sugiyama, M., Luxburg, U., Guyon, I. & Garnett, R. (eds.) *Advances in Neural Information Processing Systems*, vol. 29 (Curran Associates, Inc., 2016). URL <https://proceedings.neurips.cc/paper/2016/file/d490d7b4576290fa60eb31b5fc917ad1-Paper.pdf>.
17. Refinetti, M., d’Ascoli, S., Ohana, R. & Goldt, S. The dynamics of learning with feedback alignment. *arXiv preprint arXiv:2011.12428* (2020).
18. Launay, J., Poli, I., Boniface, F. & Krzakala, F. Direct feedback alignment scales to modern deep learning tasks and architectures. *Advances in Neural Information Processing Systems* **33** (2020).
19. Bartunov, S. *et al.* Assessing the scalability of biologically-motivated deep learning algorithms and architectures. In *Proceedings of the 32nd International Conference on Neural Information Processing Systems*, 9390–9400 (2018).
20. Launay, J., Poli, I. & Krzakala, F. Principled training of neural networks with direct feedback alignment. *arXiv preprint arXiv:1906.04554* (2019).

21. Filipovich, M. J., Cappelli, A., Hesslow, D. & Launay, J. Scaling laws beyond backpropagation. *arXiv preprint arXiv:2210.14593* (2022).
22. Saade, A. *et al.* Random projections through multiple optical scattering: Approximating kernels at the speed of light. In *2016 IEEE International Conference on Acoustics, Speech and Signal Processing (ICASSP)*, 6215–6219 (IEEE, 2016).
23. Brossollet, C. *et al.* Lighton optical processing unit: Scaling-up ai and hpc with a non von neumann co-processor. *arXiv preprint arXiv:2107.11814* (2021).
24. Launay, J. *et al.* Hardware beyond backpropagation: a photonic co-processor for direct feed-back alignment. *arXiv preprint arXiv:2012.06373* (2020).
25. Filipovich, M. J. *et al.* Silicon photonic architecture for training deep neural networks with direct feedback alignment. *Optica* **9**, 1323–1332 (2022).
26. Ohana, R., Hesslow, D., Brunner, D., Gigan, S. & Müller, K. Linear optical random projections without holography. *Opt. Express* **31**, 25881–25888 (2023). URL <https://opg.optica.org/oe/abstract.cfm?URI=oe-31-16-25881>.
27. Popoff, S. *et al.* Measuring the transmission matrix in optics: an approach to the study and control of light propagation in disordered media. *Physical review letters* **104**, 100601 (2010).
28. Drineas, P. & Mahoney, M. W. Randnla: randomized numerical linear algebra. *Communications of the ACM* **59**, 80–90 (2016).
29. Mahoney, M. W. *et al.* Randomized algorithms for matrices and data. *Foundations and Trends® in Machine Learning* **3**, 123–224 (2011).
30. Martinsson, P.-G. & Tropp, J. A. Randomized numerical linear algebra: Foundations and algorithms. *Acta Numerica* **29**, 403–572 (2020).
31. Hesslow, D. *et al.* Photonic co-processors in hpc: using lighton opus for randomized numerical linear algebra (2021). [2104.14429](https://arxiv.org/abs/2104.14429).

32. Cappelli, A., Launay, J., Meunier, L., Ohana, R. & Poli, I. Ropust: improving robustness through fine-tuning with photonic processors and synthetic gradients. *arXiv preprint arXiv:2108.04217* (2021).
33. Cappelli, A. *et al.* Adversarial robustness by design through analog computing and synthetic gradients. In *ICASSP 2022-2022 IEEE International Conference on Acoustics, Speech and Signal Processing (ICASSP)*, 3493–3497 (IEEE, 2022).
34. Ohana, R. *et al.* Photonic differential privacy with direct feedback alignment. *Advances in Neural Information Processing Systems* **34**, 22010–22020 (2021).
35. Rafayelyan, M., Dong, J., Tan, Y., Krzakala, F. & Gigan, S. Large-scale optical reservoir computing for spatiotemporal chaotic systems prediction. *Physical Review X* **10**, 041037 (2020).
36. Radford, A. *et al.* Language models are unsupervised multitask learners. *OpenAI blog* **1**, 9 (2019).
37. Danescu-Niculescu-Mizil, C. & Lee, L. Chameleons in imagined conversations: A new approach to understanding coordination of linguistic style in dialogs. *arXiv preprint arXiv:1106.3077* (2011).
38. Anderson, M. G., Ma, S.-Y., Wang, T., Wright, L. G. & McMahon, P. L. Optical transformers. *arXiv preprint arXiv:2302.10360* (2023).
39. Chowdhery, A. *et al.* Palm: Scaling language modeling with pathways. *Journal of Machine Learning Research* **24**, 1–113 (2023).
40. Watson-Parris, D. *et al.* Climatebench v1. 0: A benchmark for data-driven climate projections. *Journal of Advances in Modeling Earth Systems* **14**, e2021MS002954 (2022).
41. Nguyen, T., Brandstetter, J., Kapoor, A., Gupta, J. K. & Grover, A. Climax: A foundation model for weather and climate. *arXiv preprint arXiv:2301.10343* (2023).

42. Xu, J., Sun, X., Zhang, Z., Zhao, G. & Lin, J. Understanding and improving layer normalization. *Advances in neural information processing systems* **32** (2019).
43. Kaplan, J. *et al.* Scaling laws for neural language models. *arXiv preprint arXiv:2001.08361* (2020).